Eur. Phys. J. D **40**, 195–199 (2006)
DOI: 10.1140/epjd/e2006-00144-9

THE EUROPEAN PHYSICAL JOURNAL D

Line strength measurements for near-infrared intersystem transitions of NI

A. Bacławski[a], T. Wujec, and J. Musielok

Institute of Physics, Opole University, ul.Oleska 48, 45-052 Opole, Poland

Received 20 March 2006 / Received in final form 31 May 2006
Published online 23 June 2006 –

Abstract. Intensities of 15 intersystem transitions and 5 LS allowed multiplets of neutral nitrogen (NI) from infrared part of the spectrum were measured by emission spectroscopy method. All allowed as well as LS-forbidden spectral lines belong to the $3p$-$3d$ transition array. The nitrogen spectra were excited in a wall-stabilized high-current arc ran in helium with small admixture of nitrogen. On the basis of these line (multiplet) intensity measurements, transition probabilities of 15 intersystem lines were determined relative to transition probabilities of appropriately chosen allowed multiplets. Finally the relative data for intersystem transitions were normalized to an absolute scale by applying reference multiplet strength values recommended by the Atomic Spectroscopy Group of NIST. The determined line strengths are compared with available calculated and — in the case of 5 transitions — also with experimental data.

PACS. 32.70.Cs Oscillator strengths, lifetimes, transition moments – 32.70.Fw Absolute and relative intensities – 52.70.Kz Optical (ultraviolet, visible, infrared) measurements

1 Introduction

Spectroscopic data for LS-forbidden spectral lines are very important e.g. for astrophysical applications. Forbidden transitions appear in the spectra originating from various astronomical objects e.g.: from symbiotic stars, from different layers of the Sun [1], from planetary nebulae and from diffuse astrophysical plasmas [2]. Numerous forbidden spectral lines are used in spectroscopic diagnostics procedures for determination of temperature, electron density and abundance of various elements in these light sources. The accuracy and reliability of radiative transition probabilities for such spectral lines are thus very important, not only for testing coupling schemes in atomic systems, but also for possible applications in plasma diagnostics. LS-forbidden lines of neutral nitrogen are observed in spectra originating from high-lying atmospheric layers (dayglow) [3], from solar spectra [4] as well as from novae stars [5]. Numerous papers have been published in the last 15 years devoted to calculations of line strength (fine structure components) data of neutral nitrogen [6–14]. However, data for LS-forbidden transitions are reported only in four of them: by Hibbert et al. [6] (intermediate coupling calculations), Kurucz and Bell [7] (semiempirical data), and in two recent papers by Tachiev and Froese Fischer [12] (Breit-Pauli results) and by Tayal and Zatsarinny [13] (B-spline R-matrix approach). Experimental data for forbidden transitions in NI are reported by Goldbach and Nollez [15] and by Musielok et al. [16], for spectral lines from the UV and IR spectral region, respectively.

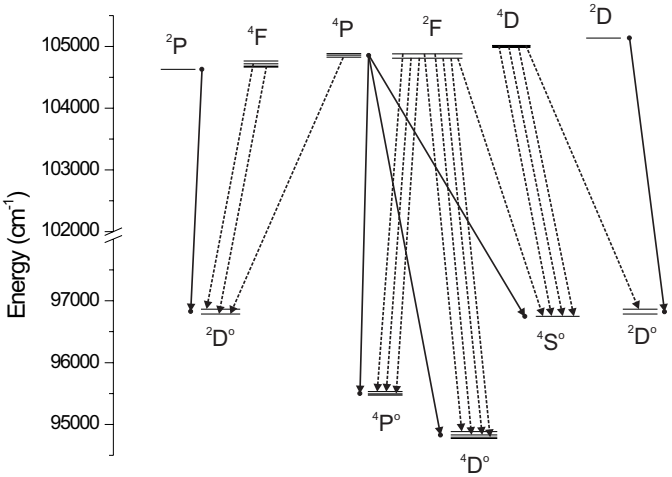

Fig. 1. Partial Grotrian diagram showing all studied $3p$-$3d$ transitions: (broken lines) LS forbidden transitions; (solid lines) reference LS allowed multiplets.

In this work we have studied 15 LS-forbidden spectral lines of NI, belonging to the transition array $3p$-$3d$, from the wavelength interval 900–1300 nm. Figure 1 shows the partial Grotrian diagram with all studied intersystem transitions (dotted lines) and LS allowed multiplets (solid lines), taken as reference data for relative intensity measurements. Eight intersystem transitions originate from

[a] e-mail: abac@uni.opole.pl

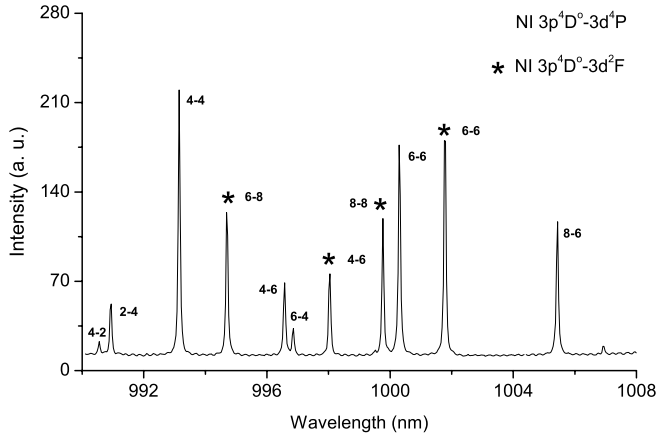

Fig. 2. The measured spectrum (after radiance calibration) in the wavelength interval 990–1008 nm is shown. The numbers in the vicinity of the fine structure components are the statistical weights of the lower and upper level of the transition, respectively. The LS forbidden lines are additionally marked with stars. The component (2-2) of the multiplet $^4\mathrm{D}^\circ - {}^4\mathrm{P}$ is missing in the figure since its wavelength is 988.336 nm. The intensity of this component is by a factor 0.43 weaker than the intensity of the line at 993.147 nm (component 4-4).

the upper term ^{2}F, four from ^{4}D, two from ^{4}F and one from ^{4}P. The studied intersystem transitions do not obey the LS selection rules $\Delta S = 0$ and $\Delta L = 0, \pm 1$.

2 Experimental and plasma diagnostics

The experimental setup applied in this work was the same as described in our previous papers devoted to the study of CI [17] and NI [18] spectra. Therefore we restrict the description of the experimental part of this work to some details concerning the registration of the NI infrared spectra and the plasma diagnostic procedure. The high-current wall-stabilized arc, described in detail in [19] was operated at 40 amps. at atmospheric pressure in helium with some admixture of nitrogen. This admixture was kept at a rather small amount in order to assure optical thin conditions for all studied NI spectral lines. The spectra were recorded applying a charge-coupled device (CCD) sensitive up to 1700 nm. Applying a tungsten strip radiation standard source, calibrated at National Institute of Standards and Technology, the radiance calibration of the whole measuring system, including the CCD detector, has been performed. In order to check for possible self-absorption of radiation along the arc column (end-on observation) the procedure described in [17] was used.

The electron density of the plasma was obtained from measured full width at half maximum (FWHM) of the violet HeI transition ($2p\ ^3\mathrm{P}^\circ - 5d\ ^3\mathrm{D}$) at 402.636 nm. The broadening of this line is dominated by the Stark effect caused by interactions of charged particles (electrons and ions) with helium atoms. In order to determine the plasma electron density the broadening parameters (electron impact width and asymmetry parameter) reported by Griem [20] were used. In this way, for our arc discharge conditions we obtained an electron density of $N_e = (3.0 \pm 0.6) \times 10^{15}\,\mathrm{cm}^{-3}$ corresponding to the arc axis. At this N_e value the assumption of statistical (Boltzmann) distribution among upper energy levels belonging to the configuration $3d$, from which the studied NI spectral lines originate (see Fig. 1), is well fulfilled. According to the criterion given by Drawin [21,22], for establishing pLTE conditions at temperatures of our arc plasma in the range 12600–15400 K (uncertainty limits of our measurements) electron densities of about $3.7 \times 10^{13}\,\mathrm{cm}^{-3}$ are sufficient for establishing Boltzmann-like distribution among the energy levels under consideration. This estimated N_e value is almost two orders of magnitude smaller than the electron density in our excitation source.

The temperature of the arc plasma (excitation temperature) was determined from the Boltzmann plot method, applying the measured intensity ratio of two NI multiplets: $3p\ ^2\mathrm{S}^\circ - 3d\ ^2\mathrm{P}$ and $3s'\ ^2\mathrm{D} - 3p'\ ^2\mathrm{D}^\circ$. The energy gap between the upper energy terms amounts 0.73 eV. For evaluation of the temperature the corresponding transition probability data of Wiese et al. [23] were used. In this way we obtained a temperature value of 14000 ± 1400 K.

3 Evaluation of the spectra

We recorded the radiation of the arc, originating from plasma layers around the arc axis only, in the following wavelength intervals: 990–1008 nm; 1060.1–1077.8 nm; 1217.0–1234.3 nm; 1227.8–1245.2 nm; and 1265.1–1282.3 nm. The wavelength interval (about 18 nm) is determined by the dimension of the detector (20 mm) and the linear dispersion at the exit focal plane of the spectrometer. For each wavelength interval at least 15 to 20 independent recordings have been performed. The spectral ranges were chosen in such a way, that simultaneously the studied NI intersystem line (lines) and the strongest (if possible all) fine structure components of appropriate allowed multiplets, belonging to the $3p$-$3d$ transition array, could be recorded.

As an example in Figure 2 the spectrum in the wavelength range 990–1008 nm (after radiance calibration) is shown. The fine structure components of the allowed ($3p\ ^4\mathrm{D}^\circ - 3d\ ^4\mathrm{P}$) and forbidden multiplets ($3p\ ^4\mathrm{D}^\circ - 3d\ ^2\mathrm{F}$), are indicated by respective statistical weights of their lower and upper levels. The forbidden transitions $^4\mathrm{D}^\circ - {}^2\mathrm{F}$ are additionally marked with stars. One fine structure component of the allowed multiplet $3p\ ^4\mathrm{D}^\circ - 3d\ ^4\mathrm{P}$ is missing in the figure, namely the transition (2-2) at $\lambda =$ 988.336 nm, which could not be detected simultaneously with all other components. However, the contribution of this line to the total multiplet intensity has been taken into account by evaluating the neighbor spectrum (towards shorter wavelength), and assuming stability conditions for the plasma source. Its intensity is by a factor 0.43 weaker than the intensity of the (4-4) transition at $\lambda = 993.147$ nm shown in the figure.

The shapes of individual spectral lines were fitted with Voigt profiles. For the fitting within a given wavelength

interval a fixed Gaussian width was used, which corresponds to the Doppler and instrumental broadening. Also the Lorentzian component (width) was kept fixed within each allowed multiplet and the respective forbidden lines. The Lorentzian width for each multiplet was determined by accurate fitting of a selected, strong and well-isolated fine structure component. Such procedure decrease substantially possible errors, which may originate from fitting of weak or slightly disturbed fine structure components.

For some reference multiplets not all fine structure components were measured. In such cases the contribution to the multiplet intensity from the "missing" component was calculated applying the results of our previous measurements reported in [18].

After radiance calibration of the recorded spectra, the intensity ratios $I_f/I_a = I_f/\sum_i I_a^i$ have been determined, involving each selected forbidden line (I_f) and all fine structure components (I_a^i) of the allowed multiplet, taken as reference quantity. Since all studied spectral transitions (allowed and forbidden) within a given wavelength interval are measured at the same time, possible long term instabilities (drifts) of the arc emission do not influence our relative line intensity measurements. Then the corresponding transition probability ratios A_f/A_a have been evaluated according to the formula (subscripts f and a indicate the forbidden line and the allowed multiplet as a whole):

$$\frac{A_f}{A_a} = \frac{I_f}{I_a}\frac{g_a\lambda_f}{g_f\lambda_a}\exp\left(\frac{E_f - E_a}{kT}\right), \qquad (1)$$

where:

- λ the wavelength of the forbidden line (mean value for the allowed multiplet),
- g the statistical weight of the upper level (term),
- E the energy of the respective upper level (term),
- k the Boltzmann constant,
- T the temperature of the plasma.

The ratios (I_f/I_a) were calculated for each exposition of the CCD detector (each measured spectrum) independently. The final value was obtained by averaging 15–20 individual ratios. At our plasma temperature the Boltzmann factor in (1) is for all pairs (forbidden line, allowed multiplet) very close to one, because of the very small excitation energy gap between the respective excited levels. Since the largest energy gap among our pairs amounts only 171 cm^{-1}, the impact of the error in temperature ($\pm$1400 K) on evaluated transition probability ratios is negligible. The largest contribution to the uncertainty of the measured ratios (10%) arises from systematical errors of the fitting procedure, since the lines appear as very narrow spectral features. The contribution arising from determination of the multiplet intensity (based on directly measured components and — in some cases — calculated from data reported in [18]) we estimate to be not larger than 10%. Other possible error sources are: possible self-absorption, and radiance calibration. The first factor we estimate to be not larger than 1.5%, the second — because of small wavelength intervals — about 1%. The standard deviation of the ratios (A_f/A_a) from the mean value was about 2%.

4 Results and discussion

In Table 1 our experimental transition probability ratios evaluated according to formula (1) are compared with results of CIV3 calculations of Hibbert et al. [6], with semiempirical data of Kurucz and Bell [7], with the recent calculations of Tachiev and Froese Fischer [12] and with experimental ratios (5 values) reported by Musielok et al. [16]. (The paper by Tayal and Zatsarinny [13] does not provide data for forbidden transitions studied in our work). In column 1 the LS-allowed reference transitions are listed, in column 2 and 3 the studied forbidden transitions and their respective wavelengths. In the next five columns our measured ratios and the data evaluated from literature are listed. The theoretical data [6,7] differ substantially from each other. Only in two cases the ratios are in good mutual agreement (the ratios quoted in the 4th and 5th rows of Tab. 1). The ratios listed in the 5th row agree also well with our measured value. Our results agree very well with all 5 arc emission measurements of Musielok et al. — the discrepancies are well within the error limits of both experiments. Our measured ratios agree well with the results of recent calculations by Tachiev and Froese Fischer [12]: nine measured ratios agree with these calculations within the uncertainty limits of our experiment and three of them only slightly exceed the error bars (rows 4, 6 and 14 in Tab. 1). Only in three cases the differences are significant, but not exceeding 45% of the measured value (7th row in Tab. 1).

The determined transition probability ratios listed in Table 1 have been subsequently converted to line strengths ratios according to the formula:

$$S_f/S_a = (g_f/g_a)\,(\lambda_f/\lambda_a)^3\,(A_f/A_a)\,, \qquad (2)$$

where g_f and g_a are the statistical weights of the upper level and upper multiplet respectively.

On the basis of respective line strength values for the allowed multiplets taken from Wiese et al. [23] the absolute scale for the forbidden transitions have been established. The results (in atomic units) are listed in Table 2. The structure of this table is similar as in Table 1 — only the second column is added containing the corresponding absolute multiplet strengths for allowed transitions, together with estimated accuracy indicated by a code letter used in NIST-tables. The uncertainties quoted in column 5 include the measurement errors and the accuracy of the reference multiplet strengths. In addition, in Figure 3, our results are compared graphically with theoretical ones. The Figure illustrates a significant improvement of the quality of calculated line strengths achieved recently. Nearly all line strength ratios obtained from calculated data reported by Tachiev and Froese Fischer agree with our measurements within $\pm$50%, while the scatter of ratios based on older calculations [6,7] is much larger. Particularly, this notable improvement of the quality of calculated data is visible in the case of the two strongest measured intersystem transitions (results presented on the right hand side of Fig. 3). These 2 ratios are normalized to the allowed multiplet $^4S^\circ - {}^4P$. In Figure 4 we

Table 1. Comparison of transition probability ratios (A_f/A_a) measured in this work with data taken from literature. In the first column the multiplet transitions are given applied as reference quantities for the forbidden spectral lines listed in column 2.

Allowed transition ($3p$-$3d$)	Forbidden transition ($3p$-$3d$)	Wavelength (nm)	A_f/A_a				
			This work	Hibbert et al. [6]	Kurucz and Bell [7]	Tachiev and Froese Fischer [12]	Musielok et al. [16]
(1)	(2)	(3)	(4)	(5)	(6)	(7)	(8)
$^4D^\circ - {}^4P$	$^4D^\circ_{5/2} - {}^2F_{7/2}$	994.707	0.27±0.05	0.16	0.29	0.24	0.25
	$^4D^\circ_{3/2} - {}^2F_{5/2}$	998.042	0.20±0.04	0.16	0.27	0.20	0.19
	$^4D^\circ_{7/2} - {}^2F_{7/2}$	999.773	0.22±0.04	0.12	1.0	0.20	0.21
	$^4D^\circ_{5/2} - {}^2F_{5/2}$	1001.78	0.55±0.10	0.12	0.12	0.43	0.52
$^4P^\circ - {}^4P$	$^4P^\circ_{5/2} - {}^2F_{7/2}$	1069.32	0.032±0.009	0.027	0.032	0.035	—
	$^4P^\circ_{3/2} - {}^2F_{5/2}$	1073.05	0.15±0.03	0.012	0.14	0.11	0.14
	$^4P^\circ_{5/2} - {}^2F_{5/2}$	1077.50	0.049±0.013	—	0.034	0.027	—
$^2D^\circ - {}^2D$	$^4S^\circ_{3/2} - {}^4D_{5/2}$	1210.66	0.20±0.04	0.30	0.014	0.17	—
	$^4S^\circ_{3/2} - {}^4D_{3/2}$	1212.46	0.25±0.05	0.47	0.019	0.21	—
	$^4S^\circ_{3/2} - {}^4D_{1/2}$	1214.22	0.11±0.02	0.39	0.010	0.11	—
$^4S^\circ - {}^4P$	$^2D^\circ_{5/2} - {}^4D_{7/2}$	1226.13	0.040±0.008	0.032	0.28	0.035	—
	$^4S^\circ_{3/2} - {}^2F_{5/2}$	1240.43	0.21±0.04	0.022	0.0054	0.14	—
	$^2D^\circ_{3/2} - {}^4P_{5/2}$	1243.84	0.34±0.07	0.031	0.0032	0.24	—
$^2D^\circ - {}^2P$	$^2D^\circ_{3/2} - {}^4F_{5/2}$	1266.22	0.20±0.04	0.14	0.74	0.15	—
	$^2D^\circ_{5/2} - {}^4F_{7/2}$	1273.07	0.17±0.05	0.13	0.87	0.13	—

Table 2. Comparison of determined NI line strengths (in atomic units) for LS-forbidden transitions (column 5) with other available data (columns 6–9). In the first column the allowed transitions are listed applied as reference quantities. In the second column the respective multiplet strengths, used for establishing the absolute line strength scale, are given.

Allowed transition ($3p$-$3d$)	S_a Ref. [23]	Forbidden transition ($3p$-$3d$)	Wavelength (nm)	S_f				
				This work	Hibbert et al. [6]	Kurucz and Bell [7]	Tachiev and Froese Fischer [12]	Musielok et al. [16]
(1)	(2)	(3)	(4)	(5)	(6)	(7)	(8)	(9)
$^4D^\circ - {}^4P$	25.6 (C+)	$^4D^\circ_{5/2} - {}^2F_{7/2}$	994.707	4.6±1.2	2.05	2.02	2.37	4.20
		$^4D^\circ_{3/2} - {}^2F_{5/2}$	998.042	2.6±0.7	1.63	1.40	1.43	2.39
		$^4D^\circ_{7/2} - {}^2F_{7/2}$	999.773	3.8±1.0	1.63	7.36	1.91	3.63
		$^4D^\circ_{5/2} - {}^2F_{5/2}$	1001.78	7.1±1.9	1.25	0.658	3.17	6.73
$^4P^\circ - {}^4P$	52.2 (B)	$^4P^\circ_{5/2} - {}^2F_{7/2}$	1069.32	1.1±0.3	1.72	1.94	1.98	—
		$^4P^\circ_{3/2} - {}^2F_{5/2}$	1073.05	3.9±0.9	0.586	6.28	4.72	3.77
		$^4P^\circ_{5/2} - {}^2F_{5/2}$	1077.50	1.3±0.4	—	1.56	1.17	—
$^2D^\circ - {}^2D$	52.1 (B)	$^4S^\circ_{3/2} - {}^4D_{5/2}$	1210.66	6.3±1.3	8.82	4.47	5.46	—
		$^4S^\circ_{3/2} - {}^4D_{3/2}$	1212.46	5.3±1.2	9.16	4.08	4.61	—
		$^4S^\circ_{3/2} - {}^4D_{1/2}$	1214.22	1.2±0.3	3.80	1.08	1.18	—
$^4S^\circ - {}^4P$	144 (C+)	$^2D^\circ_{5/2} - {}^4D_{7/2}$	1226.13	3.8±1.0	2.55	23.8	3.13	—
		$^4S^\circ_{3/2} - {}^2F_{5/2}$	1240.43	15.3±3.8	1.38	0.355	9.75	—
		$^2D^\circ_{3/2} - {}^4P_{5/2}$	1243.84	25.0±6.6	1.95	0.210	16.6	—
$^2D^\circ - {}^2P$	18.2 (B)	$^2D^\circ_{3/2} - {}^4F_{5/2}$	1266.22	3.5±0.8	2.45	2.45	3.11	—
		$^2D^\circ_{5/2} - {}^4F_{7/2}$	1273.07	4.0±1.2	2.99	3.91	3.68	—

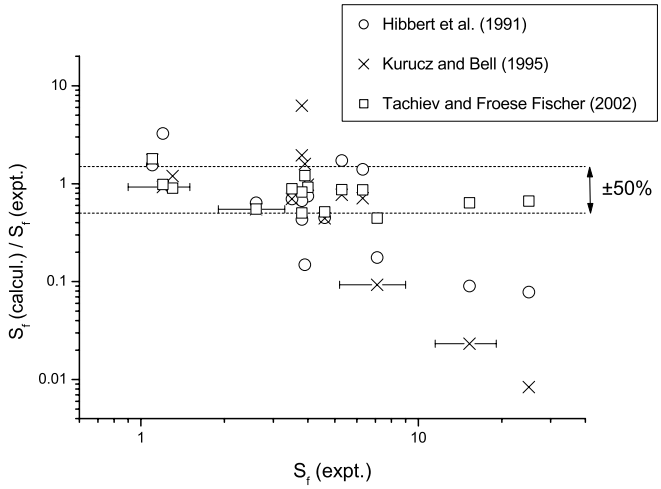

Fig. 3. Comparison of available calculated line strengths with results of our measurements. The ratios $S_{calc.}/S_{expt.}$ are plotted versus the measured line strengths (in atomic units). The figure illustrates e.g. the improvement of theoretical methods for line strength calculations.

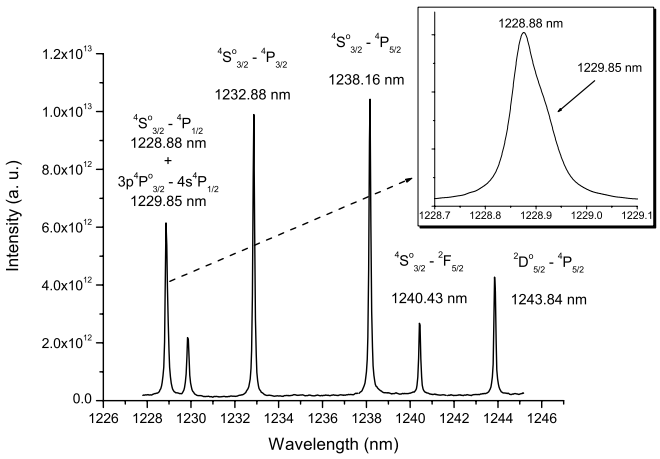

Fig. 4. The measured spectrum (after radiance calibration) in the wavelength interval 1228–1245 nm is shown. The insert presents the two overlapping lines (the stronger component belongs to the reference multiplet), taken at a better spectral resolution. For details see the text.

show the measured spectrum in the wavelength interval 1228–1245 nm, where the two above mentioned intersystem lines at $\lambda\lambda$ 1240.43 nm and 1243.84 nm appear, exhibiting the largest deviations from the older calculations. The spectrum embraces also the fine structure components of the multiplet applied as reference for establishing the absolute line strength scale. One of the fine structure components of the $^4\mathrm{S}^\circ - {}^4\mathrm{P}$ transition is blended with a line belonging to the $3p\ {}^4\mathrm{P}^\circ - 4s\ {}^4\mathrm{P}$ transition. As shown in the insert of Figure 4, the lines could be separated if the spectra were taken with a better resolution. The spectrum shown in this figure is very convincing — our measured intensities confirm the results obtained in the recent paper of Tachiev and Froese Fischer.

5 Conclusions

In the infrared part of the NI spectrum relative strong intersystem lines appear belonging to the $3p$-$3d$ transition array. The observed forbidden line strengths are of the same order of magnitude (sometimes even significantly stronger) than the allowed transitions in this wavelength interval, indicating strong violence of the LS coupling scheme. Five our measurements are in an excellent agreement with all results reported in a previous experimental study [16]. Comparison with available theoretical data shows a considerable improvement of calculated data achieved in the last few years. Recently performed calculations by Tachiev and Froese Fischer [12] are significantly more reliable than the older calculations of Hibbert et al. [6] and the semiempirical data of Kurucz and Bell [7].

References

1. T. Brage, A. Hibbert, D.S. Leckrone, Astrophys. J. **478**, 423 (1997)
2. V.H.S. Kwong, Z. Fang, T.T. Gibbons, Astrophys. J. **411**, 431 (1993)
3. R.R. Meier, Space Sci. Rev. **58**, 1 (1991)
4. G.D. Sandlin, J.-D.F. Bartoe, G.E. Brueckner, R. Tousey, M.E. van Hoosier, Astrophys. J. Suppl. Ser. **61**, 801 (1986)
5. G.S. Rossano, P. Erwin, R.C. Puetter, W.A. Feibelman, Astron. J. **107**, 1128 (1994)
6. A. Hibbert, E. Biemont, M. Godefroid, N. Vaeck, Astron. Astrophys. Suppl. Ser. **88**, 505 (1991)
7. R.L. Kurucz, B. Bell, *Atomic Line Data Kurucz CD-ROM No. 23* (Cambridge, Mass.: Smithsonian Astrophysical Observatory, 1995)
8. D.J.R. Robinson, A. Hibbert, J. Phys. B **30**, 4813 (1997)
9. S.S. Tayal, C.A. Beatty, Phys. Rev. A **59**, 3622 (1999)
10. N.W. Zheng, T. Wang, R. Yang, Y. Wu, J. Chem. Phys. **112**, 7042 (2000)
11. N.W. Zheng, T. Wang, Chem. Phys. **282**, (2002) 31
12. G.I. Tachiev, C. Froese Fischer, Astron. Astrophys. **385**, 716 (2002)
13. S.S. Tayal, O. Zatsarinny, J. Phys. B **38**, 3631 (2005)
14. S.S. Tayal, Astrophys. J. Suppl. Ser. **163**, 207 (2006)
15. C. Goldbach, G. Nollez, Astron. Astrophys. **201**, 189 (1988)
16. J. Musielok, W.L. Wiese, G. Veres, Phys. Rev. A **53**, 3588 (1995)
17. A. Bacławski, T. Wujec, J. Musielok, Phys. Scripta **64**, 314 (2001)
18. A. Bacławski, T. Wujec, J. Musielok, Phys. Scripta **65**, 28 (2002)
19. T. Wujec, A. Bacławski, A. Golly, I. Książek, Acta Phys. Pol. A **96**, 333 (1999)
20. H.R. Griem, *Spectral line broadening by plasmas* (Academic Press, New York, 1974)
21. R. Rompe, M. Steenbeck, *Progress in Plasmas and Gas Electronics* (Akademie-Verlag, Berlin 1975), Vol. 1
22. H.W. Drawin, Z. Phys. **228**, 99 (1969)
23. W.L. Wiese, J.R. Fuhr, T.M. Deters, *Atomic transition probabilities of carbon, nitrogen and oxygen: a critical data compilation* (J. Phys. Chem. Ref. Data, Monograph **7**, 1996)